MS. JULIE ZURBUCHEN (Orcid ID : 0000-0002-5275-5494)

DR. ALEX SIMMS (Orcid ID : 0000-0001-5034-2189)

Article type : Original Manuscript

A model for the growth and development of wave-dominated deltas fed by small mountainous rivers: Insights from the Elwha River delta, Washington

Julie Zurbuchen*, Alexander R. Simms*, Jonathan A. Warrick†, Ian M. Miller‡, and Andrew Ritchie§,[1]

* University of California Santa Barbara, 1006 Webb Hall, Santa Barbara, CA 93106, USA (Email: jmzurbuchen@ucsb.edu)

†U.S. Geological Survey, 400 Natural Bridges Drive, Santa Cruz, CA 95060, USA

‡Washington Sea Grant, Olympic Peninsula Field Office, 1502 E. Lauridsen Blvd. 82, Port Angeles, WA 98362, USA

§National Park Service, Olympic National Park, Port Angeles, WA 98362, USA

[1]Present address: U.S. Geological Survey, 400 Natural Bridges Drive, Santa Cruz, CA 95060, USA

Short running title: Development of small river wave-dominated deltas

Keywords [up to 6]: Elwha River delta, ground-penetrating radar, progradation, stratigraphy, swash-bar

ABSTRACT

Observations from ground-penetrating radar, sediment cores, elevation surveys and aerial imagery are used to understand the development of the Elwha River delta in north-western Washington, USA, which prograded as a result of two dam removals in late 2011. Swash-bar, foreshore and swale depositional elements are recognized within ground-penetrating radar profiles and sediment cores. A model for the growth and development of small mountainous river wave-dominated deltas is proposed based on observation of both the fluvial and deltaic settings. If enough sediment is available in the fluvial system, mouth-bars form after higher than average river discharge events, creating a large platform seaward of the subaqueous delta plain. Swash-bars form concurrently or within a month of mouth-bar deposition as a result of wave action. Fair-weather waves drive swash-bar migration landward and in the direction of littoral drift. The signature of swash-bar welding to the shoreline is landward-dipping reflections, as a result of overwash processes and slipface migration. However, most swash-bars are eroded by the river mouth, as only 10 of the 37 swash-bars that formed between August 2011 and July 2016 survived within the Elwha River delta. The swash-bars that do survive either amalgamate onto the shoreline or an earlier deposited swash-bar, forming a single larger barrier at the delta front. In asymmetrical deltas, the signature of swash-bar welding is more likely to be preserved on the downdrift side of the delta, where formation is more likely and accommodation behind newer swash-bars preserves older deposits. On small mountainous river deltas, welded swash-bars may be more indicative of a large sediment pulse to the system, rather than large hydrological events.

INTRODUCTION

Understanding modern delta morphology and stratigraphic architecture is important for accurately interpreting the sedimentary record, and enhancing scientific understanding of past depositional environments, facies heterogeneities and reservoir quality (Bhattacharya & Giosan, 2003; Ainsworth *et al.*, 2011). Wave-dominated deltas in particular typically deposit thick accumulations of well-sorted sand as deltas prograde. One important aspect of their morphology and stratigraphy is the amalgamation of swash-bars or spits onto their delta plain (Rodriguez *et al.*, 2000; Giosan *et al.*, 2005; Giosan, 2007; Anthony, 2015; Preoteasa *et al.*, 2016; Vespremeanu-Stroe *et al.*, 2016). This amalgamation is one process by which their subaerial plains prograde and is a key diagnostic feature in distinguishing wave-dominated deltas from fluvial-dominated and tidal-dominated deltas (Rodriguez *et al.*, 2000; Bhattacharya & Giosan, 2003). Once amalgamated to the shoreline, these swash-bars often form beach ridges and provide an intriguing potential for reconstructing past sediment pulses, such as large flooding events, within the evolution of the wave-dominated delta (Rodriguez *et al.*, 2000; Fraticelli, 2006).

Both mouth-bars and swash-bars are important distinguishing components of the delta plain of wave-dominated deltas (Reading, 2009). While the formation and morphology of subaerial swash-bars on modern wave-dominated deltas is well-documented in other studies (Rodriguez *et al.*, 2000; Bhattacharya & Giosan, 2003; Fraticelli, 2006; Preoteasa *et al.*, 2016; Vespremeanu-Stroe *et al.*, 2016; Nooren *et al.*, 2017), important questions remain regarding their use as sedimentary archives, including their preservation potential in the rock record. Current models are skewed toward large, near-continental scale river systems such as the Danube (Preoteasa *et al.*, 2016; Vespremeanu-Stroe *et al.*, 2016) and São Francisco (Dominguez, 1996) with bars and beach ridges that stretch alongshore at the kilometre scale. However, many active margins are riddled with small mountainous rivers that develop wave-dominated deltas whose morphology and development may be occurring at very different temporal scales.

Wave-dominated deltas are composed of a prodelta, delta front and delta plain (Reading, 2009). Depending on the depth of the receiving basin, the delta front and prodelta are the site of the most voluminous sediment deposition, with the Elwha River delta in north-west Washington being no exception (Gelfenbaum *et al.*, 2015; Ritchie *et al.*, 2018). However, the delta plain provides the subaerial portion of the delta and contains some of the most diagnostic features for distinguishing wave-dominated deltas from fluvial-dominated and tidal-dominated deltas (Bhattacharya & Giosan, 2003).

Mouth-bars form on wave-dominated deltas as fluvial outflows undergo rapid deceleration and deposit sediments (Wright, 1977). These mouth-bars are the site of the majority of the bedload deposition from the river mouth and have a large impact on the development of the tributary network within deltas (Edmonds & Slingerland, 2007). Mouth-bars often form after high-magnitude river discharge events and are subsequently reworked by wave action (Rodriguez *et al.*, 2000; Fielding *et al.*, 2005; Barnard & Warrick, 2010; Anthony, 2015). In rivers with a single point source, crescentic mouth-bars are formed (Fig 1A; Wright, 1977).

When preserved in the rock record, mouth-bars tend to have basinward dipping strata, comprised of coarsening-upward sands (Fielding *et al.*, 2005; Ainsworth *et al.*, 2016).

Another important component of the delta plains of wave-dominated deltas are swash-bars. The shore parallel, elongate sand bodies are formed by wave uprush and isolate small lagoons on their landward side (Hine, 1979; Jackson, 1997). Within the common wave-dominated delta model proposed by Wright (1977), swash-bars are largely found on top of the mouth-bar (Fig. 1B). Several studies have explored the formation of swash-bars in other prograding coastal settings, including spits and clastic shorelines (Hayes & Boothroyd, 1969; Hine, 1979; Bristow *et al.*, 2000; Lindhorst *et al.*, 2008). In these settings, storms erode sediment from the shoreface and transport it to the nearshore, where fair-weather waves rework the sediment into elongate swash-bars (Hayes & Boothroyd, 1969; Lindhorst *et al.*, 2008). The resulting internal geometry of the swash-bars consists of shallowly landward-dipping strata caused by overwash processes and slipface migration (Hine, 1979; Lindhorst *et al.*, 2008). Understanding of swash-bar development on wave-dominated deltas, with both fluvial and littoral processes playing an integral role in sediment delivery and distribution, remains limited.

The removal of two dams beginning in September 2011 along the Elwha River in north-west Washington introduced *ca* 8.2 million tonnes of sediment into the Elwha River over a two-year period (Warrick *et al.*, 2015). This removal simulated a high-magnitude river discharge event and the large increase in sediment discharge resulted in a historically unprecedented progradation of the Elwha River's wave-dominated delta (Gelfenbaum *et al.*, 2015; Magirl *et al.*, 2015; Ritchie *et al.*, 2018; Warrick *et al.*, 2019). This progradation provides a natural laboratory for recording the evolution and resulting stratigraphy of swash-bars within a small asymmetrical wave-dominated delta. The progradation of the Elwha River delta during dam removal is used to address four fundamental questions regarding the evolution of bars on wave-dominated deltas. (i) how is mouth-bar deposition related to river discharge in small mountainous river settings; (ii) does the deposition of a mouth-bar always result in the formation of a swash-bar; (iii) what is the preservation potential of swash-bars in these systems; and (iv) what is the stratigraphic record of swash-bar amalgamation on a wave-dominated delta?

In order to answer these questions, a ground-penetrating radar (GPR) survey was conducted in July 2016 to capture the stratigraphy of sediment deposited after dam removal across the modern Elwha River delta. Additionally, elevation surveys collected monthly and repeated aerial photographs since 2011 captured the changing morphology of the delta and the welding of swash-bars onto the delta plain.

BACKGROUND AND REGIONAL SETTING

Elwha River delta

The Elwha River flows north from the Olympic Mountains into the Strait of Juan de Fuca, west of Port Angeles, Washington (Fig. 2). The Olympic Mountains are an accretionary wedge formed by the convergence of the Juan de Fuca plate with the North American plate and includes assemblages of metasedimentary, sedimentary and volcanic rocks. Glacial processes shaped the landscape and deposited till and outwash that reach tens of metres thick (Downing, 1983; Warrick *et al.*, 2009). The Elwha River delta formed during a local highstand in sea level *ca* 12.5 ka, caused by the retreat of the Late Wisconsin glaciers across northern Washington State, leaving behind a depressed crust (Webster, 2014). Isostatic rebound of the glacially depressed crust caused a rapid relative fall in sea-level during which the delta prograded into the Strait of Juan de Fuca and subsequently was flooded as relative sea level in the region rose *ca* 50 m from *ca* 10 to 6 kyr before present (Downing, 1983; Mosher & Hewitt, 2004). The relict, subaqueous lowstand delta extends 2 to 5 km into the Strait and dips *ca* 1° towards the slope break (Eidam *et al.*, 2016).

The headwaters of the Elwha River reach an elevation of *ca* 1400 m and the river drops to the ocean in *ca* 70 km. Steep slopes in the watershed contribute to landslides, rockfalls and debris flows, supplying sediment to the river (Montgomery & Brandon, 2002). The Elwha River watershed drains an area of 831 km^2 and has an average sediment yield of *ca* 340 000 tonnes a^{-1} (Magirl *et al.*, 2015). The mean annual discharge of the river is 42 m^3 s^{-1} and the two-year recurrence interval flood is 400 m^3 s^{-1}, with higher flow occurring during the fall-winter storms and the spring freshets (Duda *et al.*, 2011; Eidam *et al.*, 2016). Average significant wave heights at the Elwha River delta are *ca* 0.4 m (Warrick *et al.*, 2009). Waves are dominated by north-westerly swell originating in the Pacific Ocean, and winds drive waves from the west and north-west (Warrick *et al.*, 2009). Tides near Port Angeles are mesotidal with a great diurnal tide range of 2.15 m (Warrick & Stevens, 2011).

Dam removal

The Elwha Dam, completed in 1913 at river kilometre 8, and the Glines Canyon Dam, completed in 1927 at river kilometre 22, were built on the Elwha River to supply hydroelectric power to Port Angeles, Washington. The dams captured the upper watershed supply of sands and gravels, and reduced bedload to the lower reaches of the Elwha River by *ca* 90%, starving the delta of sediment (Warrick *et al.*, 2009). By 2010, the two dams had trapped *ca* 21 million m^3 of sediment; about half of the sediment was clay and silt and the other half was sand, cobbles and boulders (Randle *et al.*, 2015). In 1992, the US Congress passed a resolution to restore the Elwha River ecosystem and fisheries and the two dams were slated for removal as part of the largest dam decommissioning in the USA to date (Duda *et al.*, 2011; Gelfenbaum *et al.*, 2015). The phased removal process began on 17 September 2011, with the Elwha Dam taking just over seven months to remove and the Glines Canyon Dam taking about three years. A full description of the dam removal process is found in Randle *et al.* (2015).

In the two years following the initiation of dam removal, *ca* 8.2 million tonnes of sediment, or 5.9 million m^3, assuming an average bulk density of 1.4 tonnes m^{-3}, was released from the reservoirs behind the dams (Gelfenbaum *et al.*, 2015; Magirl *et al.*, 2015). An estimated *ca* 6.3 million tonnes of this was suspended sediment load consisting of clay, silt and sand (Magirl *et al.*, 2015). Although most of the fine-grained sediment escaped into the Strait of Juan de Fuca, the majority of coarse-grained sediment (sand and gravel) was captured at the delta mouth and extended the active delta by nearly 200 m to the north, through the welding of bars (Gelfenbaum *et al.*, 2015; Warrick *et al.*, 2015, Warrick *et al.*, in press).

METHODOLOGY

Ground-penetrating radar

Over 10 km (91 lines) of ground-penetrating radar (GPR) profiles were collected on the Elwha River delta on 17 to 20 July 2016 (Fig. 2). The GPR provides a useful tool for imaging sediment layers and storm deposits in coastal areas (Van Heteren *et al.*, 1998; Buynevich *et al.*, 2004; Wang & Horwitz, 2007; Tamura, 2012; Hein *et al.*, 2014; Lindhorst & Schutter, 2014). The GPR data were collected using a hand-towed Sensors & Software pulseEKKO PRO GPR system (Sensors & Software Inc., Mississauga, Canada). Common-offset surveys were collected using 100 MHz, 200 MHz and 500 MHz antennas. The frequencies obtain resolutions of 0.15 m, 0.10 m and 0.03 m and penetrated to depths of up to 7 m, 5 m and 2 m, respectively. The groundwater table at the Elwha River delta is located about 1.8 m below mean sea level and penetration of the GPR signal in some areas is limited by the presence of salt or brackish water, whose high dielectric constants spread the signal. The GPR lines were collected primarily shore normal to image maximum dip angles, with 21 shore parallel lines for correlation.

Common-midpoint (CMP) surveys were conducted at both the western and eastern portions of the Elwha River delta to determine local radar velocities of the sediments. A radar velocity of *ca* 0.107 m ns^{-1} was obtained for both sides, within the range reported for previous studies of sandy coastal areas (Switzer *et al.*, 2006; Wang & Horwitz, 2007).

The GPR data were processed using Sensors & Software EkkoView Deluxe by applying dewow, automatic gain control (AGC), bandpass filter and a synthetic aperture image reconstruction migration to focus scattered signals. Elevation data were collected simultaneously using a HiPer Lite Plus RTK-GPS system (Topcon Positioning Systems Inc., Livermore, CA, USA). After processing, GPR data were topographically corrected using a simple vertical shift of traces to correct for terrain using elevations obtained from the GPS survey and the average velocity of sediments obtained from the CMP surveys. The GPR profiles were interpreted in IHS Kingdom® software using techniques discussed in Neal (2004) and Buynevich & Fitzgerald (2001). The GPR data presented in this paper are from the 500 MHz transducers which provided the highest resolution images of the delta stratigraphy.

Sediment cores

Seventeen vibracores, penetrating to depths of 0.5 to 2.4 m, were taken along the same transects as GPR profiles to ground-truth GPR interpretations (Fig. 2). Cores were split, photographed and described, noting grain size, bedding surfaces and any sedimentary structures. Grain-size analysis was conducted on samples from cores EW02, EW05 and EW07 (Figs 2 and 3) at 10 cm intervals using sieves at six grain-size intervals, ranging from -1.25 to 4 φ (2.38 mm to 62.5 μm). Mean grain size was determined from cumulative weight percent graphs (Folk & Ward, 1957). Cores were correlated to two-way travel time GPR profiles in Kingdom® using velocities from the CMP surveys to obtain the correct time/depth relationships. When GPR profiles were converted to depth, geophysically imaged stratigraphic boundaries appeared to correlate with sedimentary contacts in cores, indicating a reasonable velocity was obtained from the CMP surveys.

Topographic data and maps

The USGS collected bathymetric and topographic surveys of the Elwha River delta before, during and after dam removal (Gelfenbaum *et al.*, 2015). During the project, these data were collected biannually to capture seasonal aspects of the coastal morphodynamics as the delta grew from new sediment inputs. Methods included bathymetric measurements from single-beam sonar systems mounted to personal watercraft with differential Global Navigation Satellite Systems (GNSS) in real-time kinematic (RTK) mode and topographic measurements from RTK GNSS systems mounted on backpacks. Further details of data collection and processing are provided in Gelfenbaum *et al.* (2015) and data are provided in USGS ScienceBase (Stevens *et al.*, 2016). Additional monthly topographic surveys were collected along a single transect (164 in the USGS surveys; Fig. 2) using a pole-mounted RTK-Differential Global Positioning System (DGPS). Topographic survey data from July 2016 were used to calculate the modern slopes of the delta landforms.

Aerial orthomosaics of the Elwha River mouth were derived from National Park Service (NPS) photographic surveys conducted about every two to four weeks during the dam removal project (Ritchie, 2014; East *et al.*, 2015; Randle *et al.*, 2015; Warrick *et al.*, 2015). The 'orthophotos' were developed from 'Structure from Motion' analyses of thousands of aerial photographs per survey using Agisoft Photoscan Pro georeferenced with more than 100 ground control points around the lower 30 km of the river and 10 km of the shoreline. The 'orthophotos' taken in the study area (Fig. 2; red box) were used in combination with the topographic survey data to estimate the timing of mouth-bar deposition and swash-bar formation by the first appearance of bars.

River and ocean conditions

River discharge and turbidity data were examined to determine the influence of river discharge and sediment load on mouth-bar deposition. River discharge data were acquired from USGS gauge 12045500, located between the two removed dams (waterdata.usgs.gov last accessed on 29 January 2017) (Figs 2 and 4A). Turbidity data from USGS gauge 12046260, located below both dam sites, were used as a proxy for sediment load (waterdata.usgs.gov last accessed on 24 March 2017) (Figs 2 and 4A). Average turbidity for the Elwha River throughout the study period was *ca* 250 formazin nephelometric units (FNU) and ranged from 0 to 2850 FNU.

In addition, significant wave heights and wave direction were examined to determine the effect of waves on both mouth-bar and swash-bar formation, migration and welding. Oceanographic information was collected by two benthic tripods located east of the Elwha River mouth from December 2010 to November 2017 (Ferreira & Warrick, 2017; Glover, 2018) (Figs 2 and 4B). A 1200 kHz RDI acoustic Doppler current profiler (ADCO; RD Instruments, Poway, CA, USA) mounted to the top of the tripod recorded current and wave conditions (Foley & Warrick, 2017). Tripod A was placed about 1 km east of the Elwha River mouth, but due to exceptional sedimentation at its site in the winter of 2013, it was relocated further east and renamed Tripod D (Ferreira & Warrick, 2017) (Fig. 2). Data from both tripods have been compiled into one time series. In order to capture the full study period and storm surge, tidal data from NOAA CO-OPS Station 9444090 offshore of Port Angeles, Washington, were examined (tidesandcurrents.noaa.gov last accessed on 31 January 2017) (Figs 2, 4C and 4D). Water level data were filtered to display only the maximum water level per 24 hour period. Additionally, the predicted tide was subtracted from the observed tide to show periods of storm surge and its effect on swash-bar migration and erosion. Storm surge is defined as occurring when the observed tide is greater than the predicted tide. For the purposes of this study, significant storm surge is defined as a period where the difference is equal to or above +0.5 m.

Mouth-bar deposition and swash-bar formation timing

The timing of mouth-bar deposition and swash-bar formation was estimated using aerial photographs and elevation surveys. Mouth-bar deposition was recognized in aerial photographs by the presence of radial sand bodies at the river mouth, which appeared subaerially in photographs, but may be subaqueous during high tides (Fig. 1A). In elevation surveys, mouth-bars were recognized again by a radial shape outward from the river mouth. In addition, the mouth-bars gently slope seaward from the river mouth to the leading edge at about 0.3°, before steeply sloping at 2° into deeper water.

Swash-bar formation was recognized in aerial photography as subaerial elongate features, parallel to and at the leading edge of the delta (Fig. 1B). In elevation surveys, the swash-bars appear similarly, and have higher slopes landward than seaward. Classification of swash-bars as downdrift, updrift and centre, were based on the formation location of the swash-bar, and the direction in relation to the river mouth in the aerial photographs and elevation surveys (i.e. centre formed directly in front of the river mouth). The date of mouth-bar deposition and swash-bar formation is noted as the date it is first seen in either aerial photographs or elevation surveys, and therefore represents the latest possible date of formation (Tables 1 and 2). Mouth-bars and swash-bars may have formed and eroded in the roughly two-week time frame between each aerial photograph.

RESULTS

Radar facies and depositional elements

The GPR profiles contain five distinct radar facies distinguished by reflection configuration and continuity (Fig. 5). Sediment cores contain four sedimentary facies distinguished by grain size and sorting (Figs 3 and 6). Three different depositional elements were identified using radar profiles, sediment cores, elevation surveys and aerial photographs. These include foreshore, swash-bar and swale. Each of the depositional elements produces a distinct radar facies or facies assemblage.

Foreshore

The first radar facies, f1-be, consists of planar, seaward-dipping, parallel, continuous reflections (Fig. 5). Reflections from this facies have minimum seaward dip angles ranging from *ca* 3° to 8° and are commonly found on the seaward side of swash-bars as well as proximal to the pre-dam removal shoreline in both pre-and post-dam removal sediments (Figs 7, 8 and 9). Often within this facies, reflections are truncated and then overlain by the same facies, creating a seaward-dipping erosional contact, henceforth referred to as an erosional surface (Figs 7 and 9). Sediment cores sampling this facies contain sedimentary facies sand 1 and sand 2. Sand 1 is a poorly sorted, coarse-skewed sand with grain sizes ranging from -0.3 to 0.7 φ (0.6 to 1.2 mm) (Figs 3 and 6). Sand 2 is a poorly sorted, fine-skewed to near-symmetrical sand with grain sizes ranging from 0.3 to 1.7 φ (0.3 to 0.8 mm) (Figs 3 and 6). Cores also show possible imbricated clasts within sand 1, as well as shallowly dipping laminations within sand 2. Similar to other interpretations from coastal settings, facies f1-be is interpreted to be foreshore deposits, representing beach progradation (Van Heteren *et al.*, 1998; Bristow *et al.*, 2000; Buynevich & FitzGerald, 2001; Bristow & Pucillo, 2006; Switzer *et al.*, 2006). This interpretation is further supported by the similarity of the reflection dip angles to the current foreshore dip angles at *ca* 4° to 8°, calculated from the July 2016 topographic survey. Aerial photographs suggest that the progradation is facilitated by longshore drift of swash-bar sediments initially deposited close to the river mouth. The erosional surfaces are interpreted to be caused by wave erosion during large storms (Buynevich & FitzGerald, 2001).

Swale

The second identified radar facies, f2-ch, is characterized by highly discontinuous chaotic reflections (Fig. 5). Aerial photographs show that this facies is found in areas that are currently, or were, in swales formed behind subaerial swash-bars as the Elwha River delta prograded into the Strait of Juan de Fuca (Figs 8 and 9). Sediment cores sampling this radar facies contain a fine sand facies composed of moderately well-sorted fine sands with a mean grain size of *ca* 2.2 φ (200 µm), and an organic rich sedimentary facies containing large amounts of woody debris (Figs 3 and 6). Based on both aerial photographs and sediment cores, radar facies f2-ch is interpreted to represent swale deposits.

Swash-bar

Two additional radar facies appear on the modern swash-bars within the eastern side of the delta, and interbedded within the progradational beach deposits, facies f1-be, on the western side of the delta. The first of these is radar facies f3-ow which contains planar, steeply landward-dipping, parallel, continuous reflections (Fig. 5). The reflections of this facies have dip angles of *ca* 27° and appear on the landward side of swash-bars as well as within packages of GPR facies f1-be, progradational beach deposits (Figs 7, 8 and 9). The second radar facies that appears on swash-bars, f3a-dl, consists of shallowly landward-dipping, divergent reflections, with dip angles ranging from 3° to 5° (Fig. 5). This radar facies is often found on the seaward side of preserved swash-bars onlapping onto a bounding surface, as well as within the central portion of modern swash-bars (Figs 7 and 9). Sediments corresponding to this radar facies consist of sedimentary facies sand 1 and sand 2, composed of moderately to poorly sorted sands that generally coarsen upward within the swash-bar from sand 2 to sand 1 (Fig. 6). Aerial photographs in locations where these facies are found display evidence of overwash processes (Fig. 10) as well as landward migration of swash-bars (Fig. 11). Both radar facies are interpreted to be caused by a combination of overwash processes and slip-face migration on swash-bars (Psuty, 1965; Hine, 1979; Bristow *et al.*, 2000; Lindhorst *et al.*, 2008).

Several profiles contain reflection free areas that occur near the surface. These occur most often within GPR transects close to the active shoreline (Figs 7 and 8). Reflection free areas close to the surface are defined as radar facies, f4-hsc (Fig. 5). This facies is interpreted to indicate locations with high salt water or brackish water concentrations. Salt has high conductivity, which increases the attenuation of electromagnetic waves (Neal, 2004).

Mouth-bar morphology and formation

After dam removal, the Elwha River delta prograded seaward, facilitated by 19 episodes of mouth-bar deposition at the delta front during the study period. These bars radiated laterally out from the river mouth in a crescentic shape. The river mouth continued to migrate through the newly formed delta plain, and often formed lozenge shaped mouth-bars, as well as triangular plan-form mouth-bars, known to form from sediment pulses and wave action (Fielding *et al.*, 2005). While the exact timing of mouth-bar deposition was not captured, aerial photographs and topographic surveys were used to bracket their timing. Therefore, discharge and turbidity (a proxy for sediment load) were explored within the time frame of possible deposition. Preceding deposition of 17 of the 19 mouth-bars between August 2011 to August 2016, discharge and/or turbidity, as measured from river gauges, increased to levels above average with discharge ranging from *ca* 60 to *ca* 280 m^3 s^{-1} and turbidity from *ca* 200 to *ca* 2850 FNU, for one to five days (Fig. 4; Table 1).

Swash-bar formation and migration

A total of 37 swash-bars formed on the Elwha River delta between August 2011 and August 2016 (Table 2). The formation of swash-bars was either concurrent with or within two months mouth-bar deposition. All but three episodes of mouth-bar deposition and growth resulted in the formation of one to five swash-bars. Wave action reworked the deposits creating a wave-dominated delta morphology on the delta plain (Gelfenbaum *et al.*, 2015). Elevations of the swash-bars ranged from *ca* 3.0 to 3.75 m (relative to NAVD88, NOAA CO-OPS Station 9444090, co-ops.nos.noaa.gov; Fig. 2). Fourteen swash-bars formed near the centre of the delta and all were subsequently eroded or reworked into other deposits. Fifteen swash-bars formed on the downdrift side of the delta. Eight of the 15 swash-bars were either eroded or reworked, and seven remained preserved either in the GPR stratigraphy or morphologically as of July 2016. Of the additional eight swash-bars that formed on the updrift side of the delta, five were eroded and three remained preserved either in GPR stratigraphy or morphologically.

Of the 37 swash-bars formed during the study period, 23 formed when wave data were available. Wave direction during the study period was predominately from the north-west with a median significant wave height of 0.4 m (Fig. 12). The average significant wave heights during possible swash-bar formation periods ranged from 0.66 m to 0.39 m (Fig. 4). Twelve of the 23 swash-bars formed when significant wave heights were above the median for the study period. The average maximum daily water level in each potential formation period, derived from tidal data, also ranged from 2.44 to 1.82 m with 23 out of 37 swash-bars formed when the maximum daily water level was lower than average.

After formation, the swash-bars either remained stationary, migrated landward or were subsequently eroded by channel migration. Only two of the swash-bars in the study were completely eroded by wave action, one on the updrift side of the delta and one on the far downdrift side. Twenty-six of the 37 swash-bars migrated, moving landward towards the shoreline, with additional downdrift elongation to the east in the direction of littoral drift, often slightly narrowing the swash-bar (Fig. 11). Migration lasted on average three months but ranged from just under one month to over a year and stopped when the swash-bar amalgamated to the shoreline or when another bar formed seaward of the initial bar. As the bars migrated, they left behind a large subaqueous platform on top of the mouth-bars.

Sparse wave data captured all or part of 16 swash-bars' migration period (Fig. 4). Nine of those swash-bars migrated over a period where average significant wave heights were greater than average for the study period. Tidal data was available for the entire study period and captured all 26 migration periods. The average maximum daily water levels during migration periods ranged from 1.86 to 2.33 m and was lower than the study period average in 18 of the 26 periods. Significant storm surge occurred during ten migration periods and ranged from occurring 0.06% to 5.0% of the total time. Migration of swash-bars occurred throughout most of the study period, with notable exceptions from January to March 2014, October to February 2015 and January to March 2016.

Downdrift versus updrift stratigraphy

The updrift and downdrift sides of the Elwha River delta contain similar radar and sediment facies, yet the morphology and GPR stratigraphy of the two sides differ. At the time of the GPR survey in July 2016 the GPR stratigraphy of the updrift side of the delta was dominated by facies f1-be, or seaward-dipping foreshore and upper shoreface deposits (Fig. 7). Small packages of swash-bar facies could be distinguished within GPR profiles, as well as erosional surfaces. The topography shows one swash-bar offshore of a steeply sloping beach (*ca* 10°). The downdrift side of the delta contained a mix of foreshore, swash-bar and swale GPR facies (Figs 8 and 9), which are absent from the updrift side. Additionally, fine-grained sands and organic material are absent from the updrift side but are found in the swales and as thin beds within the swash-bars of the downdrift side. The downdrift side of the delta also has a more defined ridge and swale topography, with three swash-bars captured in the elevation surveys (Figs 8, 9 and 11).

DISCUSSION

Mouth-bar deposition

Mouth-bars often form on wave-dominated deltas after high-magnitude river discharge events, such as large floods (Fielding *et al.*, 2005; Barnard & Warrick, 2010; Anthony, 2015). At the Elwha River delta, 17 out of 19 mouth-bars were deposited after short-term increases in river discharge. However, these increases in river discharge were still lower than the two-year recurrence flood interval of 400 $m^3 s^{-1}$ and river discharge shows no significant changes before and after dam removal, so another factor likely contributed to the formation of mouth-bars. From September 2011 to July 2013 and probably beyond, the Elwha River experienced an increase in sediment supply (Magirl *et al.*, 2015). The excess sediment supplied to the Elwha River from the dam removal is comparable to the large sediment load delivered after wildfires, landslides, volcanic eruptions and typhoons (Foley *et al.*, 2015). This two or more years of sustained sediment supply from eroded sediment trapped behind the dams in the Elwha River system was enough to form mouth-bars during lower discharge than normally required in other systems or prior to dam removal. This contrasts with larger systems, such as the Danube, which are thought to form barriers only after large river discharge events (Bhattacharya & Giosan, 2003).

Not all increases in discharge in the Elwha River, however, correlated with mouth-bar deposition, including two peaks to over 200 $m^3 s^{-1}$ at the beginning of the study period in November 2011 and one in February 2015. One possible explanation for the discrepancy at the beginning of the study period is that the river needed time to fill the existing accommodation within the lower reaches of the river valley and on the subaqueous delta created after the dams were built in the early 1900s, before mouth-bars could form. Significant wave heights during this time also tend to be higher overall and recent modelling has shown that large waves can suppress mouth-bar formation (Jerolmack & Swenson, 2007; Nardin & Fagherazzi, 2012).The second, later period of high discharge not associated with mouth-bar formation may be a result of greater storm energy, but the lack of wave data precludes testing of this hypothesis. Additionally, mouth-bars may have been deposited subaqueously and at times during which the bathymetric surveys were unable to capture their deposition.

Swash-bar formation and depositional model

Previous studies of swash-bars have focused on prograding shorelines and spits, where swash-bars are thought to form after large storms reactivate sediment from the foreshore and backshore dunes, and move it offshore, where it then nucleates into a bar (Hayes & Boothroyd, 1969; Lindhorst *et al.*, 2008). However, the genesis of the swash-bars at the Elwha River delta differs in that the sediment source for the swash-bars has a direct fluvial origin. All but two swash-bars form within a month of mouth-bar deposition, and the two that form later are initially seen at lower tidal levels than their previous aerial photograph, indicating that they may have simply been subaqueous following mouth-bar deposition. The clear association of swash-bars with mouth-bar deposition in this wave-dominated delta suggests that the mouth-bars provide the sediment that is immediately reworked by waves to form swash-bars. Additionally, while high waves are known to hinder the formation of mouth-bars (Nardin & Fagherazzi, 2012), available wave data suggest that wave heights at the Elwha River delta are not large enough to hinder swash-bar formation.

After formation, the swash-bars migrate landward due to reworking of their sediments by waves. As the swash-bar migrates, it tends to thin in the shore parallel direction as it elongates downdrift. Overwash processes and slip-face migration both form the landward-dipping stratification preserved in the sedimentary record (Figs 7, 8 and 9). Swash-bars prevent waves from eroding the back-bar area, thereby preserving the bedsets that form as the swash-bar migrates landward. Migration of swash-bars occurred throughout most of the study periods except over three notable time periods. The migration did not occur during three of the winters (i.e. January to March 2014, January to March 2016 and October 2014 to February 2015), suggesting that stormier weather patterns, often more common during the winter, may inhibit migration. Significant storm surge also accompanied these periods, although wave data do not indicate higher than average significant wave heights. Migration stops when the swash-bar amalgamates to the shoreline or another swash-bar, or a swash-bar forms seaward of it, protecting it from wave action. Thus, multiple swash-bars representing multiple high discharge events are preserved as a single amalgamated swash-bar.

Two erosional surfaces were imaged in ground-penetrating radar and formed during the time period between elevation surveys taken in September 2014 and January 2015 (Figs 7 and 9). Erosion surfaces can be caused by large storms (Buynevich *et al.*, 2004), but little work has quantified how large waves must be to cause such erosion. During the time when erosion surfaces formed, at least one wave event with wave heights >1.5 m struck the delta, although a break in the wave data time series from October 2014 to December 2015 prevents further analysis. The sedimentary characteristics of deposits formed during a later period of wave activity with wave heights of >1.5 m in late 2015 was not captured in the GPR stratigraphy because of high salt-water conductivity in the area.

A simple model for the formation of swash-bars on small wave-dominated deltas is proposed (Fig. 13). After a high discharge event with enough sediment available in the system, a large mouth-bar will be deposited on the delta front. Concurrently, wave action reworks the mouth-bar sediments to form swash-bars at the leading edge of both the downdrift and updrift sides of the delta. Fair-weather wave processes dominate, and lead to the swash-bar migrating shoreward, and downdrift. As the swash-bar migrates, it leaves behind a platform created by the remaining mouth-bar sediments on the delta plain, which continues to expand seaward with subsequent discharge events. The swash-bar welds to the shoreline or stops migrating if another bar forms seaward of it following the next discharge event. Swash-bars that do not weld to the shoreline on the downdrift side of the delta continue migrating in the direction of longshore drift, with their downdrift end eventually connecting to the shoreline. Local patches of finer sediment may be preserved between the migrating swash-bar and subaqueous delta plain, such as the thin bed (*ca* 2 cm) of organic material found in core EW04 (Fig. 8). The migration of swash-bars downdrift results in beach progradation, as seen by facies f1-be. High waves may erode the shoreface, or seaward side of the swash-bars at any time during the welding process.

Swash-bar preservation potential

The preservation of the landward-dipping stratification provides a stratigraphic signature of swash-bar welding in the sediment and rock record. Elevation surveys overlain onto GPR profiles provide evidence of swash-bar migration and welding to form composite swash-bars. The stratigraphic signature of swash-bar welding within GPR can record how many bars have welded onto an existing shoreline or swash-bar to produce better records of past wave and discharge activity.

The potential for this signature to form and be preserved is dependent on the location swash-bar formation on the delta. All swash-bars formed at the centre of the river mouth on the delta were eroded by channel migration. Aerial photographs suggest that 15 swash-bars have formed on the downdrift side of the delta since dam removal. In July 2016, only three of the swash-bars were preserved or recognizable in elevation surveys and aerial photographs (Fig. 2). Aerial photographs show the erosion of swash-bar j by channel avulsion; however, swash-bar facies, f3-ow, interpreted to be from this bar are preserved in GPR (Table 2; Fig. 8). Additionally, the GPR profile from transect 164 shows evidence that swash-bar k3 is the composite of three different swash-bars welded together (Table 2, bars k3, m and v; Fig. 8). Elevation surveys provide evidence for swash-bar y further offshore on transect 164; however, GPR was unable to image sediments on this swash-bar due to salt water infiltration. Altogether, the GPR profile from transect 164 and elevation surveys recorded seven of 15 swash-bars formed on the downdrift side of the delta. Thus, due to potential erosion by the river channel or waves, the number of preserved swash-bar signatures will be a minimum estimate of the number of swash-bars that formed.

In July 2016, aerial photographs and elevation surveys show one subaerial swash-bar, bar bb, on the updrift side of the delta (Fig. 2). The GPR profiles from the updrift side of the delta contain evidence of two swash-bar welding events that occurred during the study period within the stratigraphy of the shoreface (Table 2, bars k1 and x; Fig. 7). However, aerial photographs and elevation surveys suggest that after the initiation of dam removal, at least eight subaerial swash-bars formed on the updrift side of the delta; thus at least five swash-bars were not captured in the stratigraphic record.

Two factors favoured formation and preservation of swash-bars on the downdrift side of the delta. First, littoral drift increases the sediment supplied to the downdrift side of the delta, increasing the likelihood of swash-bar formation. Second, the downdrift side of the delta develops swales that persist over several years and provide accommodation for the deposition of swash-bar overwash sediment, enhancing the preservation potential of the bar welding signature. Although swales are formed on the updrift side of the delta behind swash-bars, these areas usually disappear after several months. For the signature of swash-bar welding to be preserved, there must be sufficient time and sediment deposition between swash-bar welding and significant shoreface erosion by the prevailing wave-driven and tidally-driven currents (Warrick *et al.*, 2009; Eidam *et al.*, 2016). Additionally, channel avulsion may erode swash-bars and other sediment deposited on the delta (Gelfenbaum *et al.*, 2015). The stratigraphic record does not preserve every swash-bar that formed and may only be used to determine a minimum number of bar welding events.

At the Elwha River delta, the sediment load of the river returned to pre-dam removal levels by the end of 2016, and the delta no longer experienced periods of enhanced mouth-bar formation or extension. The swash-bars that remained preserved in the delta all were welded swash-bars that formed after earlier high discharge events. Satellite imagery reveals as of 2017, that what had initially been six swash-bars (Table 2; k3, m, v, t, w1 and y) formed by different river discharge events from October 2013 to April 2015, were all amalgamated into one large barrier on the outer edge of the downdrift side of the delta (Fig. 14). This indicates that the sediment that was added to the fluvial system by the removal of the two dams was not remobilized during a single high discharge event, because no multiyear floods occurred during the study period, or even over one season, but over several seasonally high discharge events over at least four years. This contrasts with larger deltaic systems where individual swash-bars are often thought to represent large floods and have been linked to climate cycles (Fraticelli, 2006; Tamura, 2012).

The welding of several of the swash-bars into a large barrier suggests that in small mountainous river wave-dominated deltas, the presence of several closely spaced swash-bar welding signatures in a larger barrier could be more indicative of a large sediment pulse added to the fluvial system as a result of landslides, volcanic eruptions or other sediment pulses. The new barrier developed as a result of the dam removal has similar dimensions as a vegetated ridge on the older Holocene delta plain, to the east of the current river delta (Fig. 14), suggesting that large sediment pulses may have created similar features in the past.

CONCLUSION

The sustained sediment supply following dam removal on the Elwha River delta led to the deposition of at least 19 mouth-bars following moderate increases in discharge and turbidity along the river. Within one month of initial mouth-bar deposition between one and five swash-bars formed from wave action at the leading edge of 16 of the 19 new mouth-bars. After formation the swash-bars migrated landward and in the direction of littoral drift over a period of two months to over a year, until they either welded to the shoreline or another swash-bar, or were eroded by the river channel. Within ground-penetrating radar profiles, the landward migration of these swash-bars produced landward-dipping reflections, which in the case of swash-bar welding onlaps a seaward-dipping boundary surface which separates the landward-dipping reflections from the older seaward-dipping reflections marking progradation of the older beach or swash-bar. Although the preservation potential of the swash-bar welding signature was higher on the downdrift side of the delta due to higher frequency of formation and accommodation created behind younger swash-bars, not every swash-bar survived or left a record of welding within ground-penetrating radar (GPR) profiles. Thus, this signature can only be used to infer a minimum number of swash-bar welding events that occurred on the delta.

After the initial increase in sediment load due to dam removal decreased, the continued amalgamation and wave reworking of the surviving swash-bars formed a larger barrier at the front of the delta plain. The barrier is similar in scale to older vegetated ridges on the delta plain. Although, the creation of individual new swash-bars correlates with higher than average discharge, the formation of the large barrier was not triggered by a single flood or storm, but sustained sediment supplied via normal seasonal high discharge over the course of several years. Thus, in small mountainous river deltas the amalgamation of swash-bars into a large barrier may be indicative of a large sediment pulse to the river system, rather than flooding on the river.

ACKNOWLEDGEMENTS

The authors would like to extend their sincere thanks to the USGS Coastal and Marine Geology Program and Olympic National Park for funding and resources, and the Lower Elwha Klallam Tribe for providing access and assistance during field work. Monthly shoreline survey data was supported by Washington Sea Grant with resources from Peninsula College and the USGS. We would also like to thank Dillon Osleger and Laura Reynolds for their assistance in collecting the GPR and cores used in this study. The authors gratefully acknowledge the generous educational grant from IHS for the academic use of the Kingdom® software, which greatly improved the ability to visualize and interpret GPR data. The authors would also like to thank Gary Hampson, Liviu Giosan and four anonymous reviewers for their feedback and comments which greatly improved this manuscript.

REFERENCES

Ainsworth, R.B., Vakarelov, B.K., MacEachern, J.A., Nanson, R.A., Lane, T.I., Rarity, F. and Dashtgard, S.E. (2016) Process-Driven Architectural Variability In Mouth-Bar Deposits: A Case Study From A Mixed-Process Mouth-Bar Complex, Drumheller, Alberta, Canada. *Journal of Sedimentary Research*, **86,** 512-541.

Ainsworth, R.B., Vakarelov, B.K. and Nanson, R.A. (2011) Dynamic spatial and temporal prediction of changes in depositional processes on clastic shorelines: Toward improved subsurface uncertainty reduction and management. *AAPG bulletin*, **95,** 267-297.

Anthony, E.J. (2015) Wave influence in the construction, shaping and destruction of river deltas: A review. *Marine Geology*, **361,** 53-78.

Barnard, P. and Warrick, J. (2010) Dramatic beach and nearshore morphological changes due to extreme flooding at a wave-dominated river mouth. *Marine Geology*, **271,** 131-148.

Bhattacharya, J. and Giosan, L. (2003) Wave-influenced deltas: geomorphological implications for facies reconstruction. *Sedimentology*, **50,** 187-210.

Bristow, C., Chroston, P. and Bailey, S. (2000) The structure and development of foredunes on a locally prograding coast: insights from ground-penetrating radar surveys, Norfolk, UK. *Sedimentology*, **47,** 923-944.

Bristow, C.S. and Pucillo, K. (2006) Quantifying rates of coastal progradation from sediment volume using GPR and OSL: the Holocene fill of Guichen Bay, south-east South Australia. *Sedimentology*, **53,** 769-788.

Buynevich, I., FitzGerald, D. and van Heteren, S. (2004) Sedimentary records of intense storms in Holocene barrier sequences, Maine, USA. *Marine Geology*, **210,** 135-148.

Buynevich, I. and FitzGerald, D.M. (2001) Styles of Coastal Progradation Revealed in Subsurface Records of Paraglacial Barriers: Duxbury, Massachusetts, USA. *Journal of Coastal Research***,** 194-208.

Dominguez, J. (1996) The Sao Francisco strandplain: a paradigm for wave-dominated deltas? *Geological Society, London, Special Publications*, **117,** 217-231.

Downing, J. (1983) *The coast of Puget Sound: Its processes and development*. University of Washington Press.

Duda, J.J., Warrick, J.A. and Magirl, C.S. (2011) Coastal and lower Elwha River, Washington, prior to dam removal—history, status, and defining characteristics. *Coastal Habitats of the Elwha River, Washington—Biological and Physical Patterns and Processes Prior to Dam Removal. US Geological Survey Scientific Investigations Report*, **5120,** 1-26.

East, A.E., Pess, G.R., Bountry, J.A., Magirl, C.S., Ritchie, A.C., Logan, J.B., Randle, T.J., Mastin, M.C., Minear, J.T., Duda, J.J., Liermann, M.C., McHenry, M.L., Beechie, T.J. and Shafroth, P.B. (2015) Large-scale dam removal on the Elwha River, Washington, USA: River channel and floodplain geomorphic change. *Geomorphology*, **228,** 765-786.

Edmonds, D. and Slingerland, R. (2007) Mechanics of river mouth bar formation: Implications for the morphodynamics of delta distributary networks. *Journal of Geophysical Research: Earth Surface*, **112**.

Eidam, E., Ogston, A., Nittrouer, C. and Warrick, J. (2016) Tidally dominated sediment dispersal offshore of a small mountainous river: Elwha River, Washington State. *Continental Shelf Research*, **116,** 136-148.

Ferreira, J.C.T. and Warrick, J. (2017) Oceanographic measurements obtained offshore of the Elwha River delta in coordination with the Elwha River Restoration Project, Washington, USA, 2010-2014: U.S. Geological Survey data release, https://doi.org/10.5066/F7CR5RW8.

Fielding, C.R., Trueman, J.D. and Alexander, J. (2005) Sharp-based, flood-dominated mouth bar sands from the Burdekin River Delta of northeastern Australia: extending the spectrum of mouth-bar facies, geometry, and stacking patterns. *Journal of Sedimentary Research*, **75,** 55-66.

Foley, M.M., Duda, J.J., Beirne, M.M., Paradis, R., Ritchie, A. and Warrick, J.A. (2015) Rapid water quality change in the Elwha River estuary complex during dam removal. *Limnology and Oceanography*, **60,** 1719-1732.

Foley, M.M. and Warrick, J.A. (2017) Ephemeral seafloor sedimentation during dam removal: Elwha River, Washington. *Continental Shelf Research*, **150,** 36-47.

Folk, R.L. and Ward, W.C. (1957) Brazos River bar: a study in the significance of grain size parameters. *Journal of Sedimentary Research*, **27**.

Fraticelli, C.M. (2006) Climate forcing in a wave-dominated delta: the effects of drought–flood cycles on delta progradation. *Journal of Sedimentary Research*, **76,** 1067-1076.

Gelfenbaum, G., Stevens, A.W., Miller, I., Warrick, J.A., Ogston, A.S. and Eidam, E. (2015) Large-scale dam removal on the Elwha River, Washington, USA: Coastal geomorphic change. *Geomorphology*, **246,** 649-668.

Giosan, L., E. Vespremeanu, J.P. Donnelly, J. Bhattacharya, and F. Buonaiuto (2005) River Delta Morphodynamics: Examples From the Danube Delta. In: *River Deltas: Concepts, Models, Case Studies* (Eds L. Goisan and J. Bhattacharya)*, SEPM Special Publication,* **83**, 391-410.

Giosan, L. (2007) Morphodynamic feedbacks on deltaic coasts: lessons from the wave-dominated Danube delta. In: *Proceedings of coastal sediments*, pp. 828-841.

Glover, H. (2018) Wave, temperature, salinity, turbidity data collected on a benthic tripod near the mouth of the Elwha River, WA in 2015-2017., Department of Oceanography Faculty Papers and Research, http://hdl.handle.net/1773/41649.

Hayes, M.O. and Boothroyd, J.C. (1969) Storms as modifying agents in the coastal environment. *Coastal Environments. NE Massachusetts, Department of Geology, University of Massachusetts, Amherst***,** 290-315.

Hein, C.J., FitzGerald, D.M., de Menezes, J.T., Cleary, W.J., Klein, A.H. and Albernaz, M.B. (2014) Coastal response to late-stage transgression and sea-level highstand. *Geological Society of America Bulletin*, **126,** 459-480.

Hine, A.C. (1979) Mechanisms of berm development and resulting beach growth along a barrier spit complex. *Sedimentology*, **26,** 333-351.

Jackson, J.A. (1997) swash bars. In: *Glossary of Geology* 4th edn, pp. 643. American Geological Institute, Alexandria, Virginia.

Jerolmack, D.J. and Swenson, J.B. (2007) Scaling relationships and evolution of distributary networks on wave-influenced deltas. *Geophysical Research Letters*, **34**.

Lindhorst, S., Betzler, C. and Hass, H.C. (2008) The sedimentary architecture of a Holocene barrier spit (Sylt, German Bight): Swash-bar accretion and storm erosion. *Sedimentary Geology*, **206,** 1-16.

Lindhorst, S. and Schutter, I. (2014) Polar gravel beach-ridge systems: Sedimentary architecture, genesis, and implications for climate reconstructions (South Shetland Islands/Western Antarctic Peninsula). *Geomorphology*, **221,** 187-203.

Magirl, C.S., Hilldale, R.C., Curran, C.A., Duda, J.J., Straub, T.D., Domanski, M. and Foreman, J.R. (2015) Large-scale dam removal on the Elwha River, Washington, USA: Fluvial sediment load. *Geomorphology*, **246,** 669-686.

Montgomery, D.R. and Brandon, M.T. (2002) Topographic controls on erosion rates in tectonically active mountain ranges. *Earth and Planetary Science Letters*, **201,** 481-489.

Mosher, D.C. and Hewitt, A.T. (2004) Late Quaternary deglaciation and sea-level history of eastern Juan de Fuca Strait, Cascadia. *Quaternary International*, **121,** 23-39.

Nardin, W. and Fagherazzi, S. (2012) The effect of wind waves on the development of river mouth bars. *Geophysical Research Letters*, **39**.

Neal, A. (2004) Ground-penetrating radar and its use in sedimentology: principles, problems and progress. *Earth-science reviews*, **66,** 261-330.

Nooren, K., Hoek, W.Z., Winkels, T., Huizinga, A., Van der Plicht, H., Van Dam, R.L., Van Heteren, S., Van Bergen, M.J., Prins, M.A. and Reimann, T. (2017) The Usumacinta–Grijalva beach-ridge plain in southern Mexico: a high-resolution archive of river discharge and precipitation. *Earth Surface Dynamics*, **5,** 529.

Preoteasa, L., Vespremeanu-Stroe, A., Tătui, F., Zăinescu, F., Timar-Gabor, A. and Cîrdan, I. (2016) The evolution of an asymmetric deltaic lobe (Sf. Gheorghe, Danube) in association with cyclic development of the river-mouth bar: Long-term pattern and present adaptations to human-induced sediment depletion. *Geomorphology*, **253,** 59-73.

Psuty, N.P. (1965) Beach-ridge development in Tabasco, Mexico 1. *Annals of the Association of American Geographers*, **55,** 112-124.

Randle, T.J., Bountry, J.A., Ritchie, A. and Wille, K. (2015) Large-scale dam removal on the Elwha River, Washington, USA: Erosion of reservoir sediment. *Geomorphology*, **246,** 709-728.

Reading, H.G. (2009) *Sedimentary environments: processes, facies and stratigraphy*. John Wiley & Sons.

Ritchie, A. (2014) The Elwha PlaneCam: A novel and affordable aerial survey method tracking river and shoreline evolution in high spatiotemporal resolution during the largest dam removal in history. In: *Salish Sea Ecosystem Conference,* 206, https://cedar.wwu.edu/ssec/2014ssec/Day2/206.

Ritchie, A.C., Warrick, J.A., East, A.E., Magirl, C.S., Stevens, A.W., Bountry, J.A., Randle, T.J., Curran, C.A., Hilldale, R.C. and Duda, J.J. (2018) Morphodynamic evolution following sediment release from the world's largest dam removal. *Scientific reports*, **8**, 1-13.

Rodriguez, A., Hamilton, M. and Anderson, J. (2000) Facies and evolution of the modern Brazos Delta, Texas: wave versus flood influence. *Journal of Sedimentary Research*, **70,** 283-295.

Stevens, A., Gelfenbaum, G.R., Warrick, J., Miller, I.M. and Weiner, H.M. (2016) Bathymetry, topography, and sediment grain-size data from the Elwha River delta, Washington, July 2016. In: *U.S. Geological Survey data release*, http://dx.doi.org/10.5066/F7GQ6VXX.

Switzer, A., Bristow, C. and Jones, B. (2006) Investigation of large-scale washover of a small barrier system on the southeast Australian coast using ground penetrating radar. *Sedimentary Geology*, **183,** 145-156.

Tamura, T. (2012) Beach ridges and prograded beach deposits as palaeoenvironment records. *Earth-Science Reviews*, **114,** 279-297.

Van Heteren, S., Fitzgerald, D., McKinlay, P. and Buynevich, I. (1998) Radar facies of paraglacial barrier systems: coastal New England, USA. *Sedimentology*, **45,** 181-200.

Vespremeanu-Stroe, A., Preoteasa, L., Zăinescu, F., Rotaru, S., Croitoru, L. and Timar-Gabor, A. (2016) Formation of Danube delta beach ridge plains and signatures in morphology. *Quaternary International*, **415**, 268-285.

Wang, P. and Horwitz, M.H. (2007) Erosional and depositional characteristics of regional overwash deposits caused by multiple hurricanes. *Sedimentology*, **54,** 545-564.

Warrick, J.A., Bountry, J.A., East, A.E., Magirl, C.S., Randle, T.J., Gelfenbaum, G., Ritchie, A.C., Pess, G.R., Leung, V. and Duda, J.J. (2015) Large-scale dam removal on the Elwha River, Washington, USA: source-to-sink sediment budget and synthesis. *Geomorphology*, **246,** 729-750.

Warrick, J.A., George, D.A., Gelfenbaum, G., Ruggiero, P., Kaminsky, G.M. and Beirne, M. (2009) Beach morphology and change along the mixed grain-size delta of the dammed Elwha River, Washington. *Geomorphology*, **111,** 136-148.

Warrick, J.A. and Stevens, A.W. (2011) A buoyant plume adjacent to a headland—Observations of the Elwha River plume. *Continental Shelf Research*, **31,** 85-97.

Warrick J.A., Stevens, A.W., Miller, I.M., Harrison, S.R., Ritchie, A.C., Gelfenbaum, G. (2019) World's largest dam removal reverses coastal erosion, *Scientific Reports*, **9**, 1-12.

Webster, K.L. (2014) *Sediment dispersal and accumulation in an insular sea: deltas of Puget Sound*, University of Washington, PhD Dissertation, 158 pp.

Wright, L. (1977) Sediment transport and deposition at river mouths: a synthesis. *Geological Society of America Bulletin*, **88,** 857-868.

FIGURE CAPTIONS:

Figure 1. (A) Schematic of mouth-bar deposition, and aerial image showing how the authors distinguished a mouth-bar. (B) Swash-bar schematic and aerial image showing how authors distinguished swash-bars (schematic drawing by Scott Condon, and photographs by A. Ritchie).

Figure 2. Satellite photograph of the Elwha River delta from July 2016 displaying locations of GPR transects as yellow lines and vibracore locations as black circles. Red GPR lines and white-outlined vibracores are discussed in the text. Image modified from Google Earth™. Inset map displays triangles at locations of USGS river gauges, diamonds at NOAA's National Data Buoy Center station PTAW1 and benthic tripods 'A' and 'D', and locations of removed dams. The red box refers to the location of the study area in the main image.

Figure 3. Vibracores EW_05 and EW_07 showing corresponding mean grain size, sorting and skewness in phi. Grain-size statistics were calculated according to Folk & Ward (1957).

Figure 4. Time series of river and ocean data from August 2011 to August 2016. (A) Red lines indicate the date of observed mouth-bar deposition, with numbers indicating the event name. Blue lines indicate the date of observed swash-bar formation, with letters indicating event name. Grey lines show the dates of aerial photographs and elevation surveys that were used to constrain bar formation timing. (B) Elwha River discharge from USGS 12045500 and turbidity from USGS 12046260. (C) Significant wave heights from benthic tripods 'A' and 'D' located east of the Elwha River delta mouth. Pink asterisks indicate the weekly average. (D) Maximum daily

water level data from NOAA CO-OPS Station 9444090 offshore Port Angeles, WA. (E) Difference in observed and predicted water levels from NOAA CO-OPS Station 9444090 offshore Port Angeles, Washington. (F) Horizontal position of mean high water along the Elwha River delta shoreline at transect 164, with the 11 February 2011 shoreline as the zero-horizontal position. Black dots indicate dates that swash-bars formed on transect 164.

Table 1. Comparison of different variables influencing mouth-bar deposition.

Table 2. Comparison of different variables influencing swash-bar formation. N/A indicates that data was unavailable for that time period. Bold letters indicate swash-bars that are preserved in the stratigraphic or geomorphic record.

Figure 5. Radar facies identified within GPR profiles and their interpreted depositional element. All figures have vertical exaggeration of 6.5x.

Figure 6. Sedimentary facies identified within vibracores.

Figure 7. Ground-penetrating radar (GPR) profile from updrift side of Elwha River delta (see Fig. 2 for location) with interpretation of same line below. (A) GPR profile with water table marked by dashed blue line. (B) Interpreted GPR profile with depositional elements overlain, sediments deposited before dam removal are shown landward of the dashed pink line and sediments deposits after dam removal are seaward of the dashed pink line.

Figure 8. Ground-penetrating radar (GPR) profile from downdrift side of Elwha River delta (see Fig. 2 for location) with interpretation of same line below. (A) Uninterpreted GPR profile. (B) Interpreted GPR profile with depositional elements overlain. All data lie above the groundwater table. Cores are shown with their corresponding sedimentary facies. Topographic profiles are overlain showing the amalgamation of three different mouth-bars as interpreted from aerial photographs, topographic profiles and radar facies f3-ow and f3a-dl. Each bar is numbered with its corresponding number from Table 2.

Figure 9. Ground-penetrating radar (GPR) profile from downdrift side of Elwha River delta (see Fig. 2 for location) with interpretation of same line below. All data lie above the groundwater table. (A) Uninterpreted GPR profile. (B) Interpreted GPR profile with depositional elements overlain. Cores are shown with their corresponding sedimentary facies.

Figure 10. (A) Aerial photograph showing overwash from storm waves occurring on the Elwha Delta in December 2015. (B) Photograph from July 2016 showing landward dipping beds on the landward side of a swash-bar (photographs by A. Ritchie and A. Simms).

Figure 11. (A) Aerial photographs showing the formation and landward migration of elongate swash-bars on the Elwha River delta from March 2014 to August 2014. Solid red lines show the location of the swash-bar in the current frame, red dashed lines show the swash-bar locations from the previous frame. Black line shows the location of transect 164. (B) Topographic profiles along transect 164 showing the landward migration of the same swash-bar from March 2014 to August 2014 (photographs by A. Ritchie).

Figure 12. (A) Histogram of significant wave heights from benthic tripods ‘A’ and ‘D’ from August 2011 to October 2014. (B) Rose diagram showing dominant wave direction at benthic tripods ‘A’ and ‘D’.

Figure 13. Schematic model for swash-bar welding on a delta. (A) The initial delta starved of sediment. (B) A mouth-bar is deposited at the delta front. (C) Wave action on the mouth-bar reworks sediments, forming swash-bars on both the updrift and downdrift edges of the delta, on top of the mouth-bar. (D). Wave action continues to rework the sediments of the swash-bars, causing migration landward and downdrift in the direction of littoral drift. Swash-bars have landward-dipping bedding on their landward side. The platform created by the mouth-bar remains intact. (E) The swash-bars become welded onto the shoreface, with landward-dipping bedding preserved as evidence of their landward migration. (F) The cycle continues, with another mouth-bar deposited on the delta, and swash-bars forming on top (schematic model drawn by Scott Condon).

Figure 14. Satellite image from Google Earth™ showing delta morphology 30 July 2017, displaying the amalgamation of bars k3, m, v, t, w1 and y into the outer barrier on the delta, as well as a relict barrier on the older Holocene delta.

Table 1. Mouth-bar deposition variables (FNU = formazin nephelometric units)

Date	**Mouth bar deposition**	**Discharge peak (m^3/s)**	**Turbidity peak (FNU)**	**Average significant wave height (m)**	**Average maximum daily water level (m)**
10.08.2012	1	156	1030	N.A	2.03
24.12.2012	2	213	1420	0.66	2.43
16.01.2013	2a	175	1330	0.51	2.17
13.02.2013	3	N.A	814	0.49	1.97
14.03.2013	4	N.A	1400	0.43	1.89
16.04.2013	5	115	1420	0.39	1.90
15.05.2013	6	152	1420	0.48	1.82
23.10.2013	7	282	2820	N.A	1.89
21.02.2014	8	232	2190	0.48	2.01
24.03.2014	9	278	2850	0.62	1.79
14.05.2014	10	111	790	0.46	2.07
16.07.2014	11	–	–	0.51	2.22
10.11.2014	12	211	1200	0.41	2.11
30.12.2014	13	282	1500	N.A	2.36
27.01.2015	14	167	687	N.A	2.05
09.04.2015	15	88	362	N.A	1.97
03.07.2015	16	–	–	N.A	2.05
19.12.2015	17	278	1490	0.55	2.44
02.02.2016	18	282	1490	0.31	2.32
04.07.2016	19	63	217	N.A	2.03

Table 2. Swash-bar formation variables

Date (formed between)	Swash bar name	Location	Average significant wave height (m)	Average maximum daily water level (m)	Migration length (months)	Average significant wave height during migration (m)	Average maximum daily water level during migration (m)	% of time migration time with significant storm surge	Current status
27.11.12 – 24.12.12	a	Centre	0.66	2.43	–	–	–	–	Eroded
24.12.12 – 16.01.13	b	Updrift	0.51	2.17	3 months	0.55	1.96	0.00	Welded to shoreline; later eroded by waves
24.12.12 – 16.01.13	b1	Downdrift	0.51	2.17	–	–	–	–	Welded to shoreline; later eroded by waves
16.01.13 – 13.02.13	c	Centre/updrift	0.49	1.97	2–3 months	0.55	1.89	0.00	Eroded
16.01.13 – 05.02.13	d	Downdrift	0.49	1.97	3–4 months	0.51	1.89	0.00	Welded to shoreline
27.03.13 – 16.04.13	e	Centre	0.39	1.90	1 month	0.43	1.86	0.00	Eroded
16.04.13 – 30.04.13	f	Centre	0.48	1.80	–	–	–	–	Eroded
30.04.13 – 15.05.13	g	Downdrift	0.48	1.82	4 months	0.45	1.98	0.00	Innermost bar on downdrift side
15.05.13 – 31.05.13	h	Centre	0.41	1.97	–	–	–	–	Eroded
28.06.13 – 26.08.13	i	Centre	0.46	2.00	3 months	0.42 (30.06–04.09)	1.97	0.00	Eroded
28.06.13 – 26.08.13	j	Downdrift	0.46	2.00	3 months	0.42 (30.06–04.09)	1.97	0.00	Eroded
19.09.13 – 23.10.13	k1	Updrift	N/A	1.89	18 months	N/A	2.03	0.66	Welded to shoreline
19.09.13 – 23.10.13	k2	Updrift	N/A	1.89	–	–	–	–	Eroded
19.09.13 – 23.10.13	k3	Downdrift	N/A	1.89	4 months	0.44 (12.12–01.02)	1.97	0.06	Middle bar on downdrift side
19.09.13 – 23.10.13	k4	Downdrift	N/A	1.89	2 months	N/A	1.94	0.09	Eroded
19.09.13 – 23.10.13	k5	Downdrift	N/A	1.89	2 months	N/A	1.94	0.09	Welded to shoreline
01.02.14 – 21.02.14	l	Downdrift	0.48	2.01	–	–	–	–	Eroded
24.03.14 – 10.04.14	m	Downdrift	0.37	2.00	8–9 months	0.41	2.03	1.03	Welded to k3

						(24.03–16.10)			
14.05.14 – 06.06.14	n	Center/updrift	0.40	1.98	1–2 months	0.42	1.99	0.00	Eroded
14.05.14 – 06.06.14	o	Centre	0.40	1.98	3–4 months	0.40	1.98	0.00	Eroded
09.07.14 – 16.07.14	p	Centre	0.51	2.22	1 month	0.44	2.01	0.00	Eroded
30.09.14 – 10.11.14	q	Updrift	0.41 (30.09–16.10)	2.11	–	–	–	–	Eroded
30.09.14 – 10.11.14	r	Centre	0.41 (30.09–16.10)	2.11	–	–	–	–	Eroded
30.12.14 – 16.01.15	s	Centre	N/A	2.05	–	–	–	–	Overtaken by sediments from u
30.12.14 – 16.01.15	t	Downdrift	N/A	2.05	–	–	–	–	Overtaken by sediment from v
27.01.15 – 16.02.15	u	Centre	N/A	2.17	–	–	–	–	Eroded
27.01.15 – 16.02.15	v	Downdrift	N/A	2.17	–	–	–	–	Welded to k3
16.02.15 – 03.03.15	w	Centre	N/A	1.92	1 month	N/A	1.88	0.00	Eroded
16.02.15 – 03.03.15	w1	Downdrift	N/A	1.92	1–2 months	N/A	1.91	0.00	Overtaken by sediments from y
09.04.15 – 16.04.15	x	Updrift	N/A	1.85	4 months	N/A	2.01	0.00	Welds to shoreline
09.04.15 – 16.04.15	y	Downdrift	N/A	1.85	5 months	N/A	2.00	0.93	Outermost bar on downdrift side
04.06.15 – 03.07.15	z	Downdrift	N/A	2.05	4–7 months	N/A	2.02	0.00	Eroded
11.12.15 – 19.12.15	aa	Centre	0.55	2.44	1 month	0.50	2.33	4.44	Eroded
16.03.16 – 01.04.16	bb	Updrift	0.42	1.89	2–3 months	0.40 (16.03–12.05)	1.91	0.00	Outer bar on updrift side
16.03.16 – 01.04.16	cc	Downdrift	0.42	1.89	2–3 months	0.40 (16.03–12.05)	1.91	0.00	Outer bar of near mouth

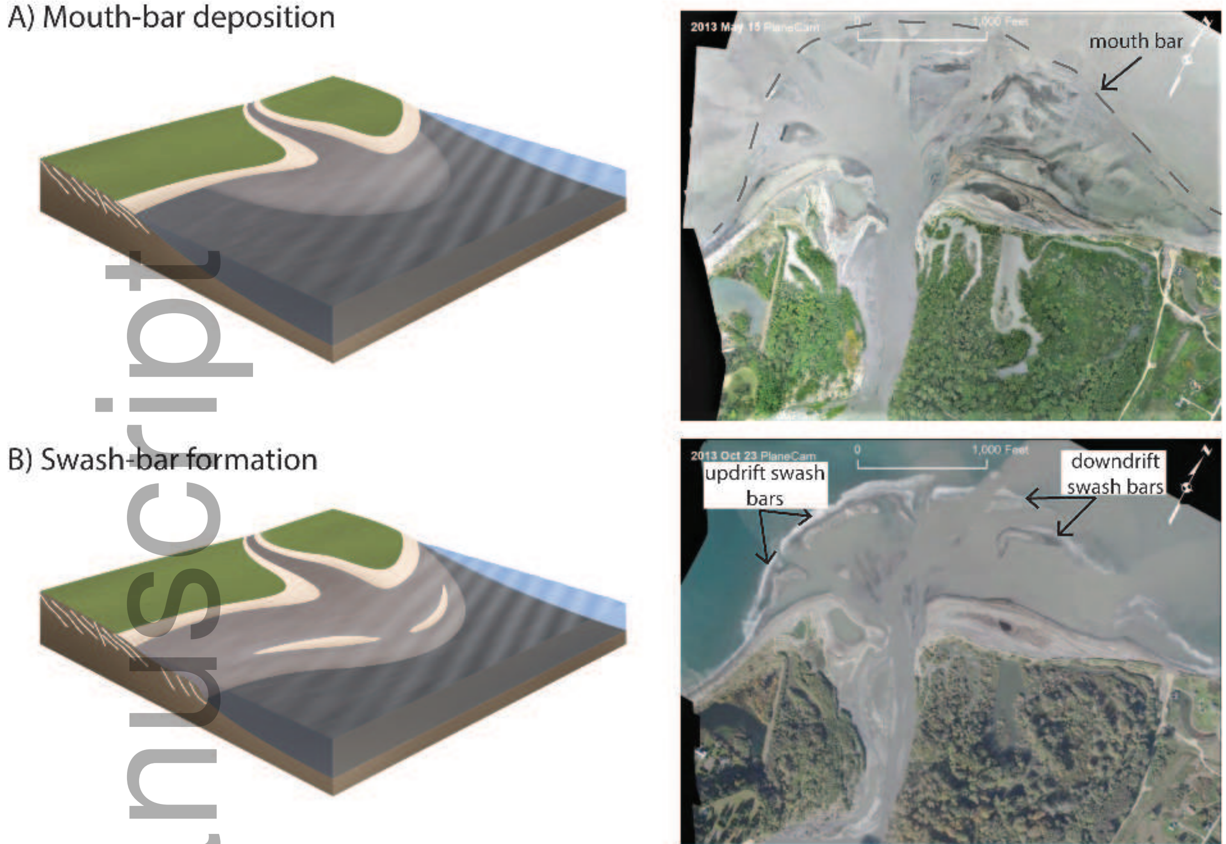

sed_12702_f1.tif

sed_12702_f2.tif

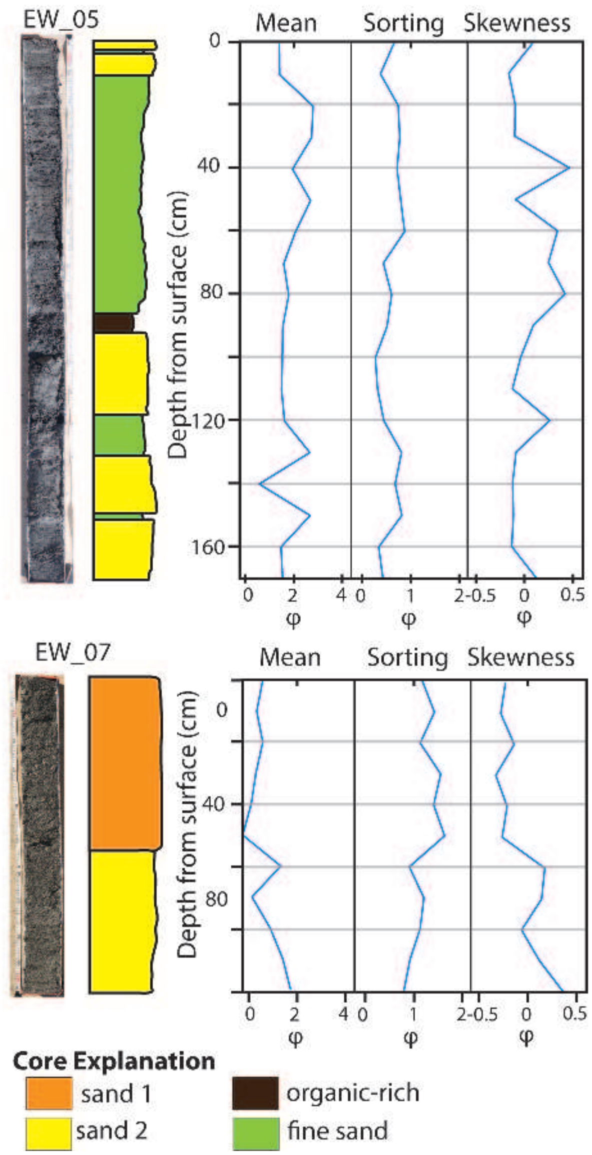

sed_12702_f3.tif

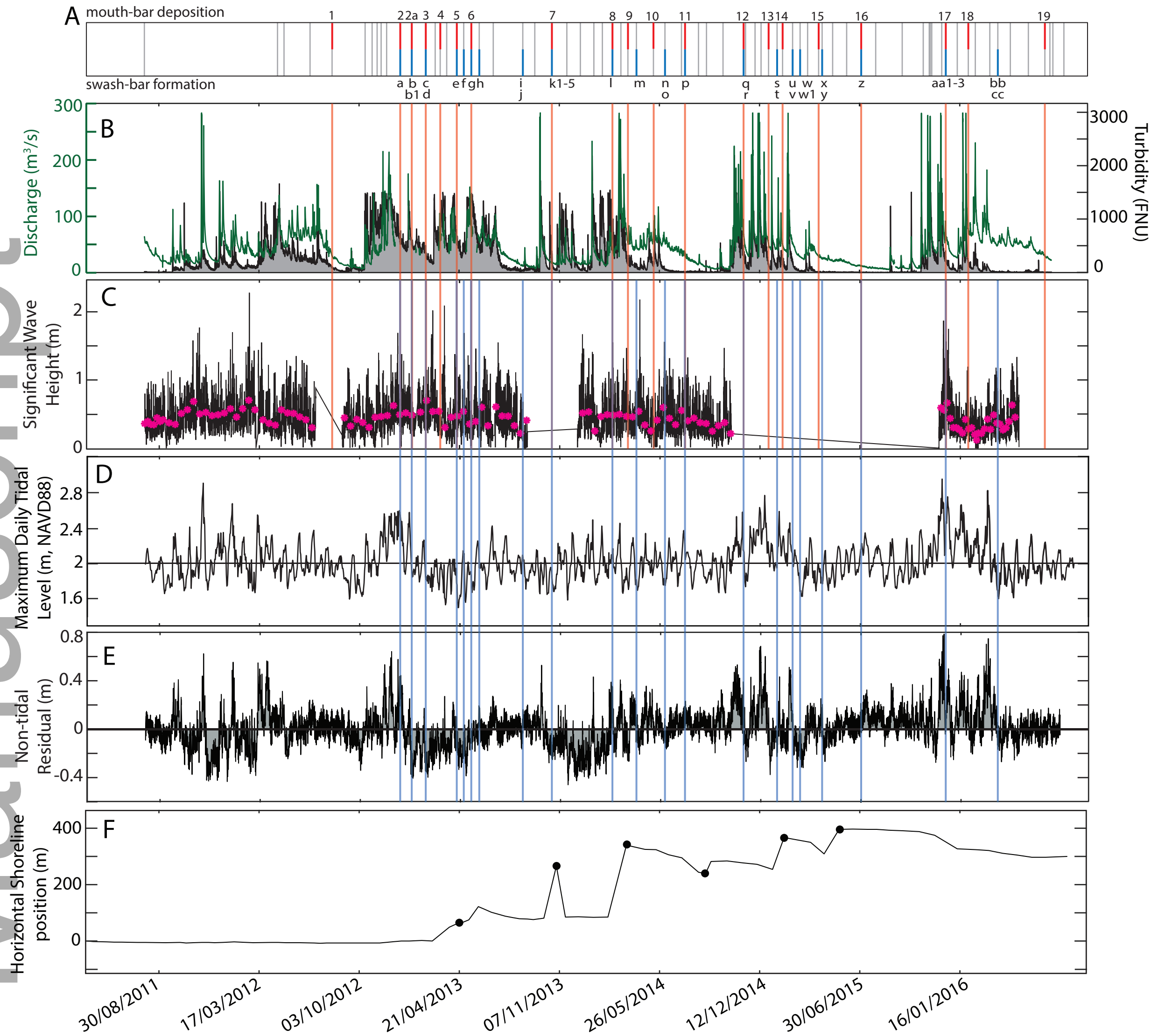

sed_12702_f4.eps

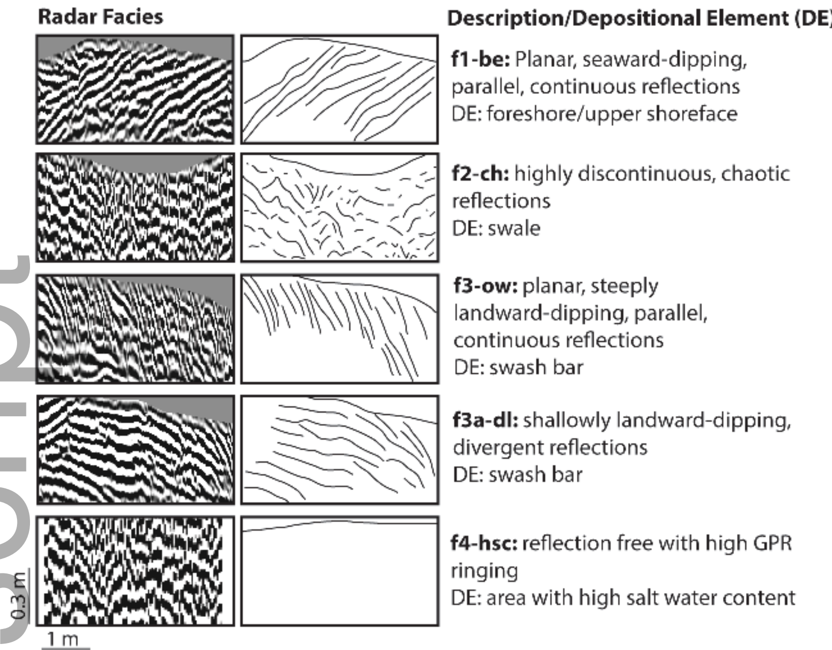

sed_12702_f5.tif

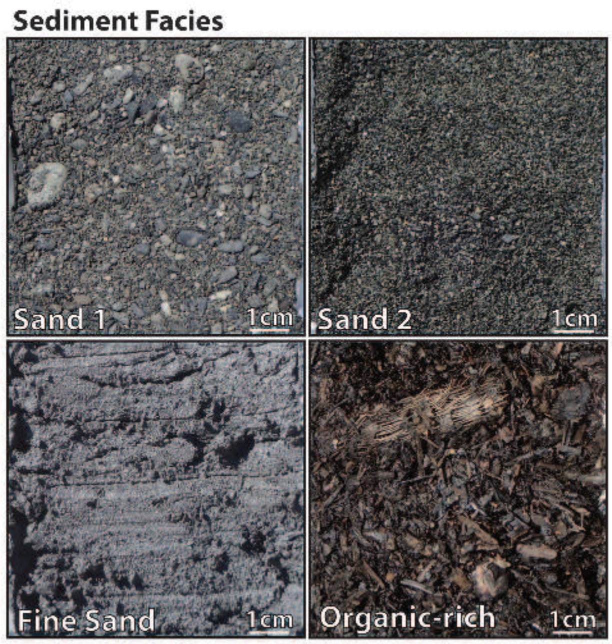

Sand 1: Poorly sorted sand, coarse skewed, with mean grain sizes ranging from -0.3 to 0.7 φ (0.6 to 1.2 mm), and clasts as large as -4.5 φ (2 cm); *Depositional element: foreshore, swash bars*
Sand 2: Moderately to poorly sorted sand, fine skewed to near symmetrical, with mean grain sizes ranging from 0.3 to 1.7 φ (0.3 to 0.8 mm); *Depositional element: foreshore, swash bars*
Fine sand: Moderately well sorted fine sands, near symmetrical, with mean grain size of 2.2 φ (200µm); *Depositional element: swale*
Organic-rich: woody debris; *Depositional element: swale*

sed_12702_f6.tif

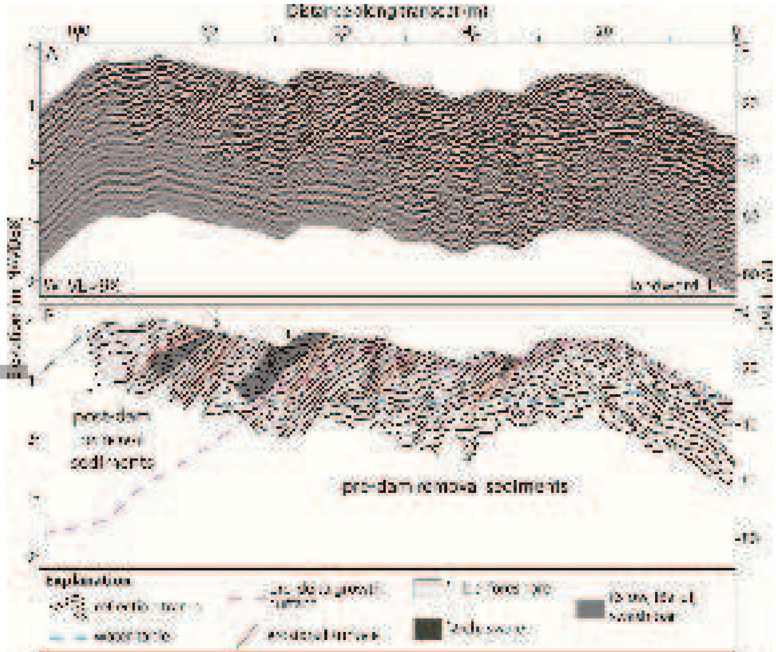

sed_12702_f7.tif

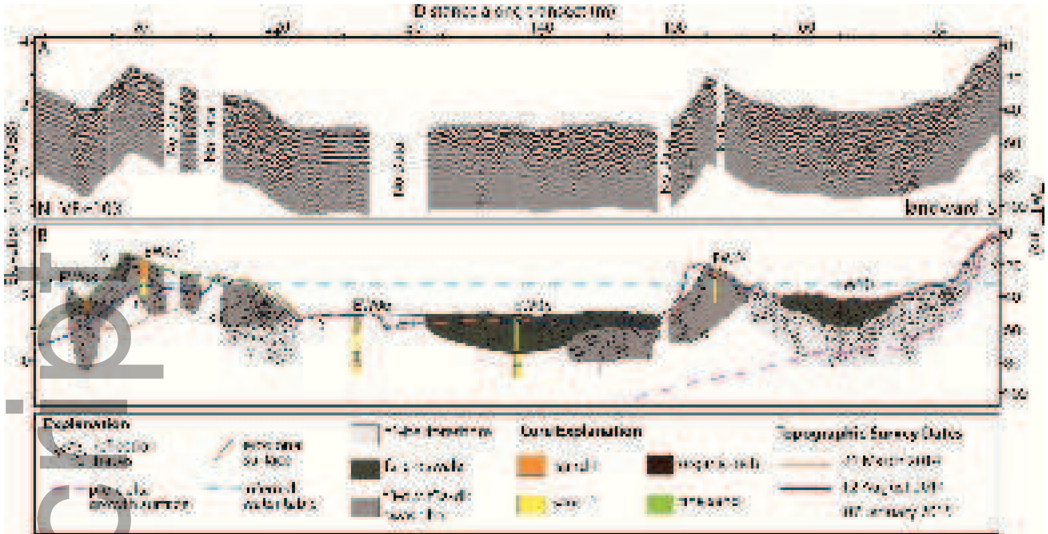

sed_12702_f8.tif

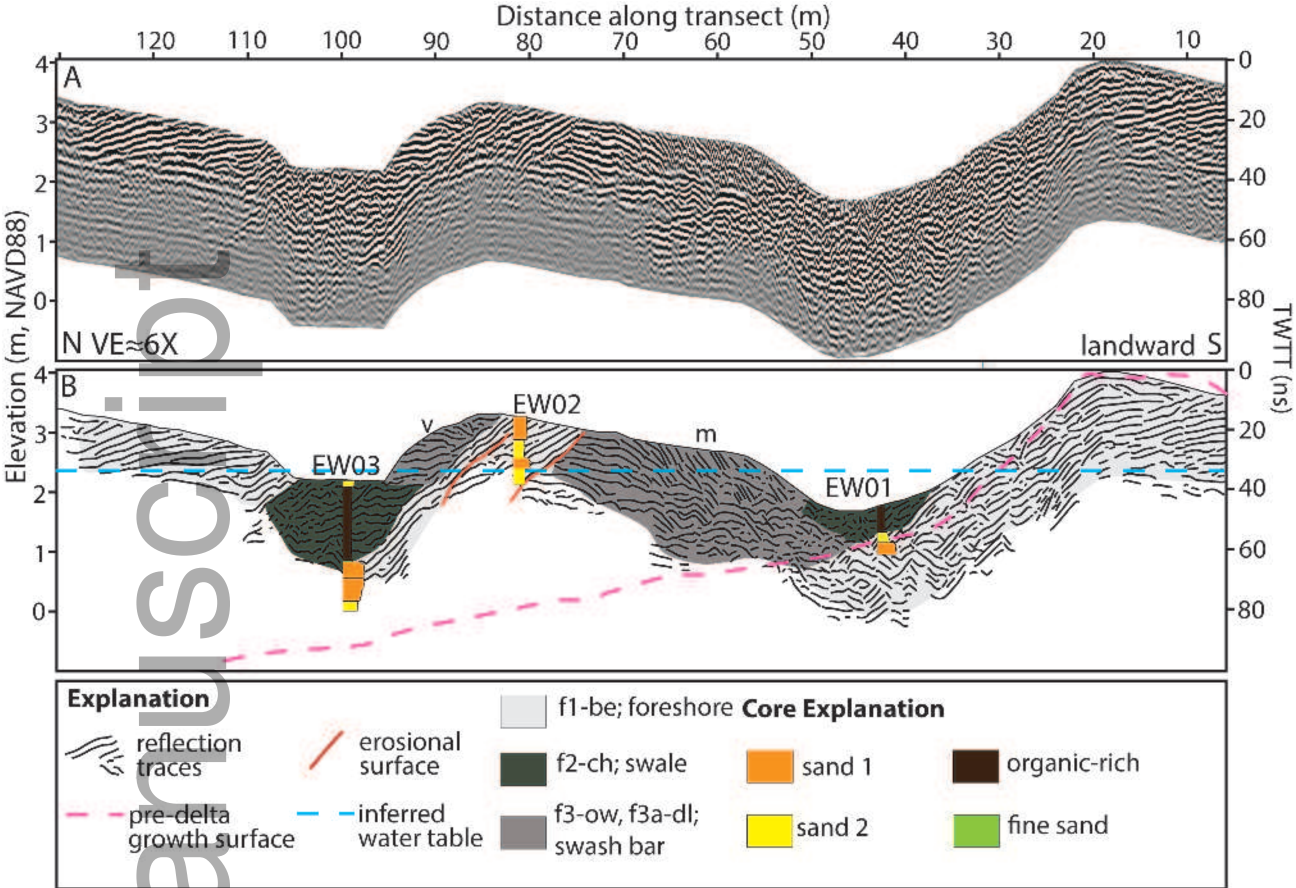

sed_12702_f9.tif

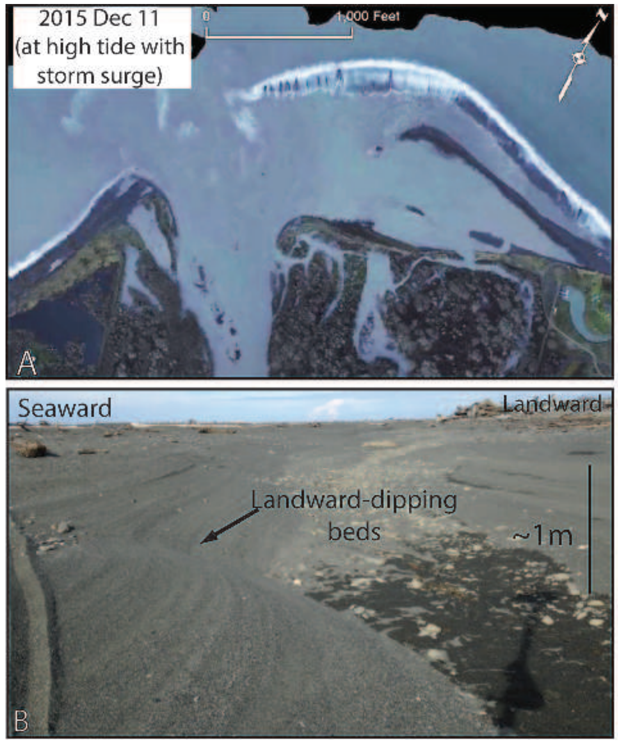

sed_12702_f10.tif

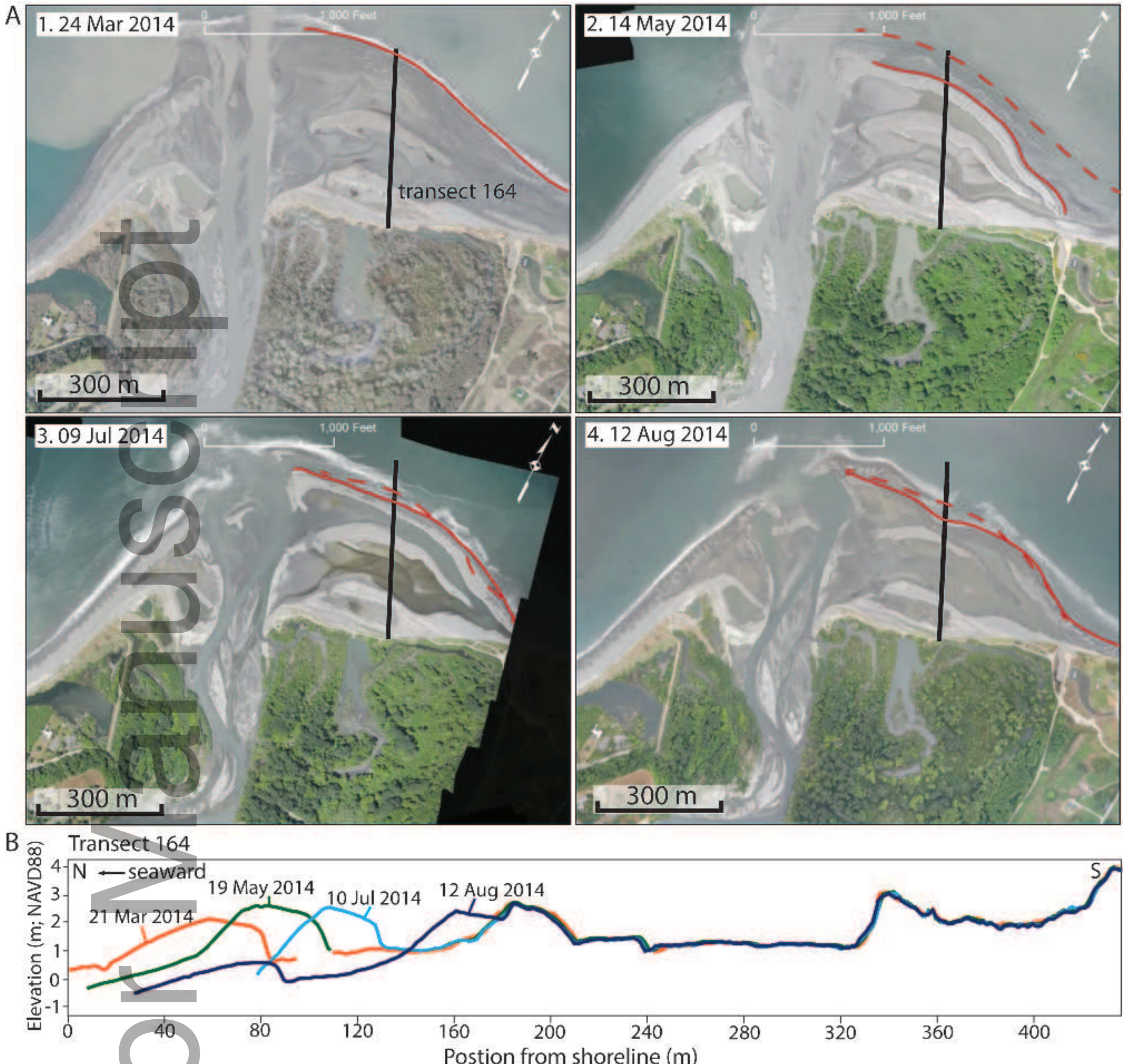

sed_12702_f11.tif

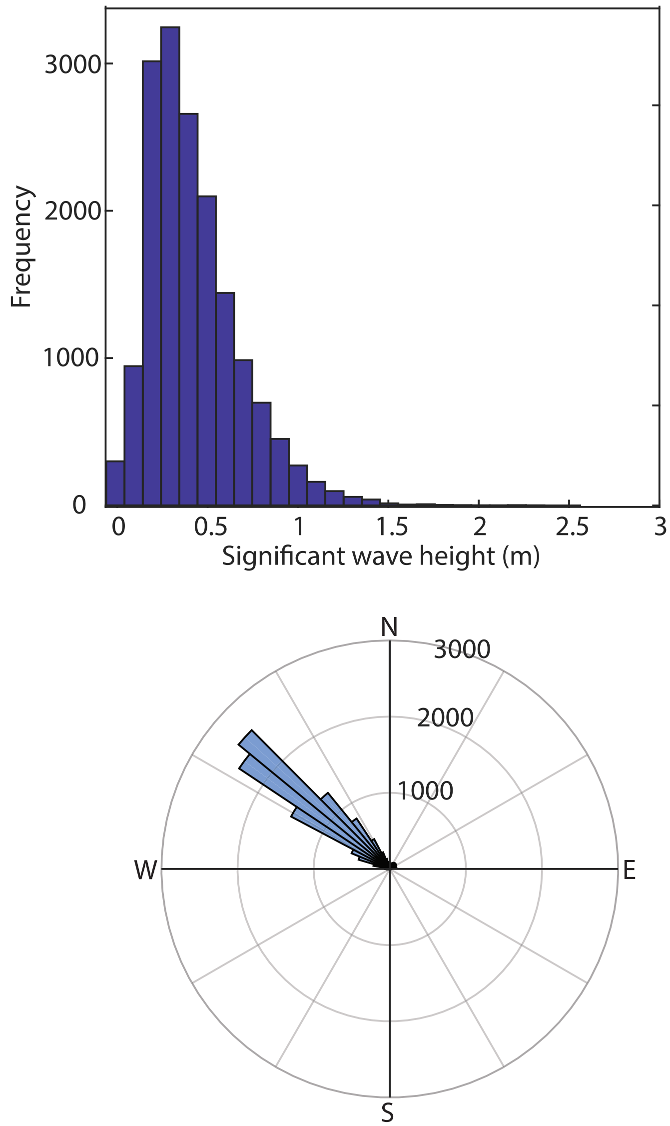

sed_12702_f12.eps

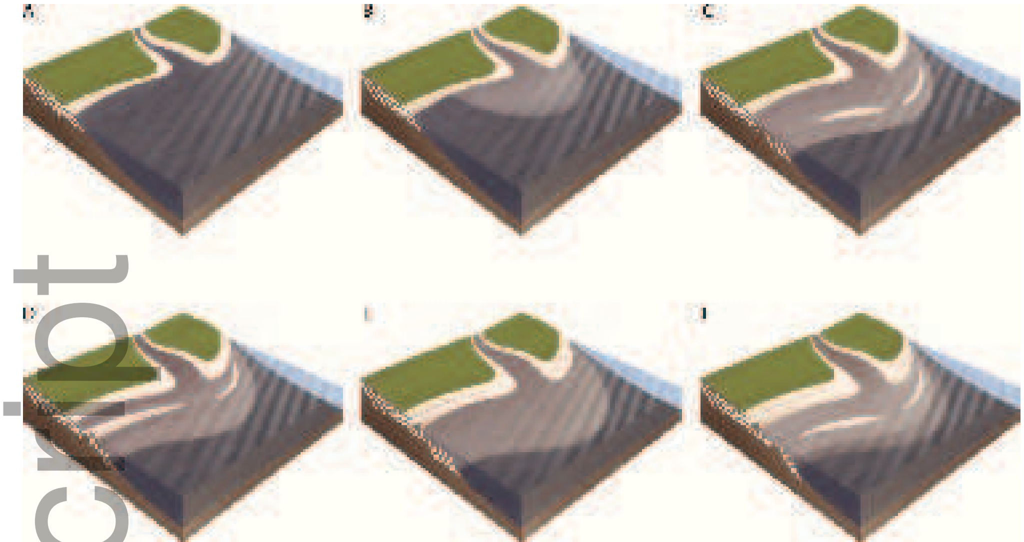

sed_12702_f13.tif

sed_12702_f14.tif